

Direct Observation of Radical Intermediates in Protein-Dependent DNA Charge Transport

Hans-Achim Wagenknecht, Scott R. Rajski, Matthias Pascaly, Eric D. A. Stemp,[†] and Jacqueline K. Barton*

Contribution from the Division of Chemistry and Chemical Engineering, California Institute of Technology, Pasadena, California 91125

Received November 16, 2000

Abstract: Charge migration through the DNA base stack has been probed both spectroscopically, to observe the formation of radical intermediates, and biochemically, to assess irreversible oxidative DNA damage. Charge transport and radical trapping were examined in DNA assemblies in the presence of a site-specifically bound methyltransferase *HhaI* mutant and an intercalating ruthenium photooxidant using the flash-quench technique. The methyltransferase mutant, which can flip out a base and insert a tryptophan side chain within the DNA cavity, is found to activate long-range hole transfer through the base pair stack. Protein-dependent DNA charge transport is observed over 50 Å with guanine radicals formed $> 10^6$ s⁻¹; hole transport through DNA over this distance is not rate-limiting. Given the time scale and distance regime, such protein-dependent DNA charge transport chemistry requires consideration physiologically.

DNA charge transport chemistry has been the subject of considerable interest with possible consequences in areas as diverse as mutagenesis and molecular electronics.^{1–4} Double helical DNA furthermore provides a unique focus for fundamental studies of charge transport through π -stacked arrays. Charge migration through the base stack has been shown to result in oxidative damage to guanine sites 200 Å from the site of a remotely bound oxidant,^{5,6} and this long-range oxidative damage is sensitive to intervening DNA sequence and structure.^{7,8} Spectroscopic studies have been utilized to probe mechanistically how DNA charge transport proceeds,^{9,10} whether through hole hopping, tunneling, or some combination thereof.¹¹

Studies in our laboratory have underscored the exquisite sensitivity of DNA-mediated charge transport to π -stacking of the donor, acceptor, and intervening base pairs.^{9,12} It is notable that spectroscopic efforts have focused on charge transport over very short distances, (10–20 Å), while biochemical measurements of oxidative damage have explored distance regimes from 30 to 200 Å. Here, for the first time, we probe charge migration through DNA assemblies both biochemically and spectroscopically so as to follow the formation of transient intermediates involved in effecting oxidative damage.

We have focused on charge migration and radical trapping in DNA assemblies in the presence of the site-specifically bound methyltransferase, *HhaI*. The enzyme carries out its alkylation chemistry after flipping out the central cytosine of its target sequence 5'-GCGC-3' and inserting a glutamine side chain of residue 237 into the resultant DNA pocket; the enzyme bound to its target site has been examined crystallographically, and the biochemistry of the wild-type enzyme as well as that of various mutants has been extensively characterized.¹³ In a DNA assembly containing a covalently tethered metallointercalator as photooxidant ([Rh(phi)₂bpy]³⁺; phi = 9,10-phenanthrenequinone diimine) and a 5'-GG-3' doublet,¹⁴ site-specific binding of the wild-type enzyme between the oxidant and its guanine target served to inhibit long-range oxidative damage.¹⁵ Moreover, binding of a Q237W mutant, which may insert the aromatic tryptophan side chain into the DNA pocket upon base

* To whom correspondence should be addressed.

[†] Department of Physical Sciences and Mathematics, Mount St. Mary's College, Los Angeles, CA 90049.

(1) Kelley, S. O.; Barton, J. K. *Metal Ions Biol.* **1999**, *36*, 211; Núñez, M.; Barton, J. K. *Curr. Opin. Chem. Biol.* **2000**, *4*, 199; Schuster, G. B.; *Acc. Chem. Res.* **2000**, *33*, 253.

(2) Fink, H.-W.; Schönenberger, C. *Nature* **1999**, *398*, 407; Porath, D.; Bezryadin, A.; de Vries, S.; Dekker, C. *Nature* **2000**, *403*, 635.

(3) Odom, D. T.; Dill, E. A.; Barton, J. K. *Chem. Biol.* **2000**, *7*, 475.

(4) Boon, E. M.; Ceres, D. M.; Drummond, T. G.; Hill, M. G.; Barton, J. K. *Nature Biotechnol.* **2000**, *18*, 1096.

(5) Núñez, M. E.; Hall, D. B.; Barton, J. K. *Chem. Biol.* **1999**, *6*, 85; Hall, D. B.; Holmlin, R. E.; Barton, J. K. *Nature* **1996**, *382*, 731.

(6) Ly, D.; Sani, L.; Schuster, G. B. *J. Am. Chem. Soc.* **1999**, *121*, 9400; Gasper, S. M.; Schuster, G. B. *J. Am. Chem. Soc.* **1997**, *119*, 12762; Henderson, P. T.; Jones, D.; Hampikian, G.; Kan, Y. Z.; Schuster, G. B. *Proc. Natl. Acad. Sci. U.S.A.*, **1999**, *96*, 8353.

(7) Giese, B.; Wessely, S.; Spormann, M.; Lindemann, U.; Meggers, E.; Michel-Beyerle, M. E. *Angew. Chem., Int. Ed.* **1999**, *38*, 996; Meggers, E.; Michel-Beyerle, M. E.; Giese, B. *J. Am. Chem. Soc.* **1998**, *120*, 12950; Giese, B. *Acc. Chem. Res.* **2000**, *33*, 631.

(8) Williams, T. T.; Odom, D. T.; Barton, J. K. *J. Am. Chem. Soc.* **2000**, *122*, 9048.

(9) Kelley, S. O.; Barton, J. K. *Science* **1999**, *283*, 375; C. Wan. Fiebig, T.; Kelley, S. O.; Treadway, C. R.; Barton, J. K.; A. H. Zewail. *Proc. Natl. Acad. Sci. U.S.A.* **1999**, *96*, 6014; Wan, C.; Fiebig, T.; Schiemann, O.; Barton, J. K.; Zewail, A. H. In press.

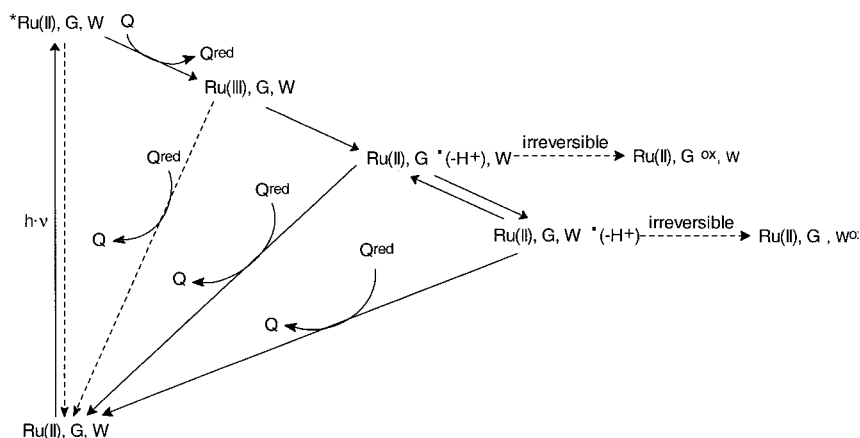
(10) Lewis, F. D.; Wu, T.; Zhang, Y.; Letsinger, R. L.; Greenfield, S. R.; Wasielewski, M. R. *Science* **1997**, *277*, 673; Lewis, F. D.; Liu, X. Y.; Liu, J. Q.; Miller, S. E.; Hayes, R. T.; Wasielewski, M. R. *Nature* **1999**, *406*, 51; Lewis, F. D.; Wu, T.; Liu, X. Y.; Letsinger, R. L.; Greenfield, S. R.; Miller, S. E.; Wasielewski, M. R. *J. Am. Chem. Soc.* **2000**, *122*, 2889.

(11) Nitzan, A.; Jortner, J.; Wilkie, J.; Burin, A. L.; Ratner, M. A. *J. Phys. Chem. B* **2000**, *104*, 5661; Jortner, J.; Bixon, M.; Langenbacher, T.; Michel-Beyerle, M. E. *Proc. Natl. Acad. Sci. U.S.A.* **1998**, *95*, 12759; Priyadarshy, S.; Risser, S. M.; Beratan, D. N. *JBIC* **1998**, *3*, 196; Felts, A. K.; Pollard, W. T.; Freisner, R. A. *J. Phys. Chem.* **1995**, *99*, 2929.

(12) Kelley, S. O.; Holmlin, R. E.; Stemp, E. D. A.; Barton, J. K. *J. Am. Chem. Soc.* **1997**, *119*, 9861; Kelley, S. O.; Barton, J. K. *Chem. Biol.* **1998**, *5*, 413.

(13) Roberts, R. J.; Cheng, X. *Annu. Rev. Biochem.* **1998**, *67*, 181–98; Cheng, X.; Kumar, S.; Posfai, J.; Pflugrath, J. W.; Roberts, R. J. *Cell* **1993**, *74*, 299; Klimasauskas, S.; Kumar, S.; Roberts, R. J.; Cheng, X. *Cell* **1994**, *76*, 357; O'Gara, M.; Klimasauskas, S.; Roberts, R. J.; Cheng, X. *J. Mol. Biol.* **1996**, *261*, 634–645; Mi, S.; Alonso, D.; Roberts, R. J. *Nucleic Acids Res.* **1995**, *23*, 620–627.

Scheme 1. Flash-Quench Reaction (G = Guanine, G^{ox} = Oxidized Guanine Products, Q = Quencher, Q^{red} = Reductive State of Q , W = DNA-Bound Trp, W^{ox} = Oxidized Trp Products)^d



^dExcitation of intercalated $[Ru(phen)_2(dppz)]^{2+}$ with visible light produces the corresponding excited ruthenium complex, $[^*Ru(phen)_2(dppz)]^{2+}$, which can be quenched via electron transfer to a nonintercalating quencher, such as $[Ru(NH_3)_6]^{3+}$, to yield the ground-state oxidant $[Ru(phen)_2(dppz)]^{3+}$. Ground state $[Ru(phen)_2(dppz)]^{3+}$ can undergo back electron transfer with the reduced quencher or can oxidize guanines within the DNA double helix. Owing to the particularly low pK_a of the guanine cation radical within the C:G base pair, only the neutral deprotonated guanine radical has been detected spectroscopically in double-helical DNA.¹⁷ At this point, the guanine radical has two fates. It can either be reduced by quencher to regenerate the whole redox system, or can oxidize a peptide side chain in the DNA π -stack, such as Trp or Tyr.^{19,20} Like the guanine radical, the Trp radical can also be reduced by the reduced quencher, yielding the regenerated system. Both radicals can undergo trapping reactions. Permanent guanine damage yields piperidine labile strand lesions which can be visualized by gel electrophoretic methods using ³²P-labeled DNA strands.

flipping, instead served to restore long-range damage. These results illustrated the key requirement of π -stacking along the path for DNA charge transport and also exemplified how DNA-binding proteins might play a role both as inhibitor and activator.

Hole transport is initiated in DNA assemblies by activation of a bound ruthenium intercalator using the flash-quench technique (Scheme 1). The flash-quench technique, developed first to explore electron-transfer reactions in proteins,¹⁶ has been employed to generate and monitor spectroscopically guanine radicals in duplex DNA¹⁷ and to promote oxidative DNA damage.¹⁸ Using the flash-quench technique, we had observed also the formation of tryptophan and tyrosine radicals in DNA upon the addition of DNA-bound peptides Lys-Trp-Lys and Lys-Tyr-Lys to ruthenated DNA assemblies;^{19,20} The irreversible products, formed upon reaction of these peptide radicals with DNA, were isolated and characterized using HPLC and mass spectrometry.

Here we describe the construction of protein/DNA assemblies containing tethered ruthenium intercalator and their application to characterize radical intermediates in long-range oxidative damage to DNA. Using a combination of gel electrophoretic assays and transient spectroscopy, we are able to correlate the formation of radical intermediates in DNA with the resultant irreversible damage to the DNA duplex. Furthermore these data allow limits to be defined concerning the time scale for charge transport through the DNA helix.

(14) The 5'-G of 5'-GG-3' is preferentially oxidized. Sugiyama, H.; Saito, I. *J. Am. Chem. Soc.* **1996**, *118*, 7063–7066; Saito, I.; Nakamura, T.; Nakatani, K.; Yoshioka, Y.; Yamaguchi, K.; Sugiyama, H. *J. Am. Chem. Soc.* **1998**, *120*, 12686; Prat, F.; Houk, K. N.; Foote, C. S. *J. Am. Chem. Soc.* **1998**, *120*, 845.

(15) Rajski, S. R.; Kumar, S.; Roberts, R. J.; Barton, J. K. *J. Am. Chem. Soc.* **1999**, *121*, 5615.

(16) I.-J. Chang, Gray, H. B.; Winkler, J. R. *J. Am. Chem. Soc.* **1991**, *113*, 7056.

(17) Stemp, E. D. A.; Arkin, M. R.; Barton, J. K. *J. Am. Chem. Soc.* **1997**, *119*, 2921.

(18) Arkin, M. R.; Stemp, E. D. A.; Pulver, S. C.; Barton, J. K. *Chem. Biol.* **1997**, *4*, 389.

(19) Wagenknecht, H.-A.; Stemp, E. D. A.; Barton, J. K. *J. Am. Chem. Soc.* **2000**, *122*, 1.

(20) Wagenknecht, H.-A.; Stemp, E. D. A.; Barton, J. K. *Biochemistry* **2000**, *39*, 5483.

Experimental Section

Materials. The oligonucleotides were prepared on an Applied Biosystems 394 DNA synthesizer using standard phosphoramidite chemistry.²¹ The ruthenated DNA oligonucleotides were prepared using the racemic tris(heteroleptic) complex, synthesized according to general methods.²² The two isomers of $[Ru(bpy')(dppz)(phen)]^{2+}$ (with the carboxylate arm axial or equatorial to the dppz ligand) were not separated. Both metal complex isomers were conjugated to the DNA oligonucleotide by a solid-phase methodology and purified as described earlier.²³ The Ru-DNA conjugates were characterized by UV/vis spectroscopy and MALDI-TOF mass spectrometry. The single strands were lyophilized and quantitated by their absorbance at 260 nm. Duplexes were formed by heating to 90 °C a solution containing equal concentrations of the complementary strands in 10 mM Tris, 1 mM EDTA, pH 8, for a period of 5 min followed by slow cooling to 25 °C over a time period of 3 h. Methyltransferases were generously provided by R. Roberts (New England Biolabs).

Laser Spectroscopy. Time-resolved emission and transient absorption measurements used an excimer-pumped dye (Coumarin 480) laser ($\lambda = 480$ nm) or a YAG-OPO laser ($\lambda_{exc} = 470$ nm).¹⁷ Laser powers ranged from 1 to 2.5 mJ/pulse. The emission of the dppz complexes was monitored at 610 nm, and the emission intensities were obtained by integrating under the decay curve for the luminescence.

Methods. DNA-protein binding conditions were as described.¹⁵ For gel electrophoresis studies of oxidative damage, all samples contained 25 mM NH_4OAc (pH 9.0), 1 mM KP_i (pH 7.4), 5 mM NaCl, 50 μM EDTA, 5% glycerol, 200 nM SAH, and a 40-fold molar excess (in base pairs) of poly(dA)-poly(dT) as nonspecific competitor DNA. Following 10 min binding at ambient temperature, samples were brought to 2 μM $[Ru(NH_3)_6]^{3+}$ and then immediately irradiated at $\lambda = 436$ nm. Following irradiation, samples were brought to a volume of 100 μL in 1 M piperidine and heated to 85 °C for 30 min. Upon completion of 1 M piperidine digestion, samples were frozen at -80 °C and lyophilized for 10 h. Samples were resuspended in loading dye (0.025% bromo-

(21) Beaucage, S. L.; Caruthers, M. H. *Tetrahedron Lett.* **1981**, *22*, 1859; Goodchild, J. *Bioconjugate Chem.* **1990**, *1*, 165.

(22) Strouse, G. F.; Anderson, P. A.; Schoonover, J. R.; Meyer, T. J.; Keene, F. R. *Inorg. Chem.* **1992**, *31*, 3004; Anderson, P. A.; Deacon, G. B.; Haarman, K. H.; Keene, F. R.; Meyer, T. J.; Reitsma, D. A.; Skelton, B. W.; Strouse, G. F.; Thomas, N. C.; Treadway, J. A.; White, A. H. *Inorg. Chem.* **1995**, *34*, 6145.

(23) Holmlin, R. E.; Dandliker, P. J.; Barton, J. K. *Bioconjugate Chem.* **1999**, *10*, 1122.

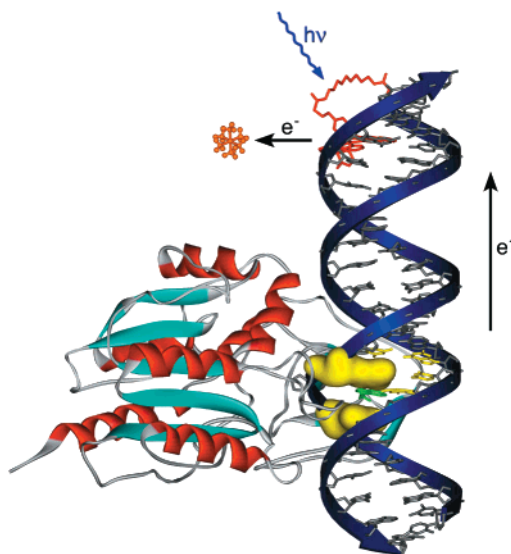


Figure 1. Protein–DNA assembly and path for DNA-mediated charge transport. The schematic shows the methyltransferase *HhaI* bound to the sequence 3′-CGXG-5′ (yellow). In a base-flipping process, the apurinic site X is rotated out of the double helix. The mutant Q237W inserts a tryptophan side chain and leaves the overall structure of the DNA without significant distortions. The ruthenium complex [Ru(bpy)-(dppz)(phen)]²⁺ (red) is shown tethered to the duplex terminus, with the dppz ligand intercalated into the DNA π -stack. The photoexcited ruthenium(II) is quenched by the nonintercalating [Ru(NH₃)₆]³⁺ (orange), generating the Ru(III) oxidant in situ. The electrochemical potential of this complex is sufficiently high to enable electron transfer from the intercalated tryptophan residue or its surrounding guanine bases (yellow surfaces).

phenol blue, 0.025% xylene cyanol in formamide) to a specific activity of 10 000 cpm/ μ L, and electrophoresis was conducted on 40 000 cpm per lane. Digestion instead with enzymes which recognize damaged sites, such as formamidopyrimidine glycosylase, have been carried out and give proportional results. Data were analyzed by phosphorimaging and ImageQuant software. Gel-shift analyses of protein–DNA complexes, 200 nM in duplex DNA with [Q237W] varied from 100 to 800 nM, were also carried out to establish binding affinity. Binding reactions were conducted in 25 mM NH₄OAc, 2mM KP_i (pH 7.4), 10 mM NaCl, 0.1 mM EDTA, 5% glycerol in the presence of 40-fold molar excess polydA-polydT.

Results and Discussion

Design of Protein–DNA Assembly with Tethered Photooxidant. Figure 1 illustrates the general protein/DNA assembly constructed and the path for charge transport being described. Figure 2 shows the specific ruthenated DNA assembly **Ru-1** used to explore radical intermediates and oxidative damage generated using the flash-quench technique as a function of binding of both the wild type and mutant methylase *HhaI*. Oxidative damage is visualized by phosphorimaging after piperidine digestion and denaturing gel electrophoresis of the strand radioactively tagged at its 5′-end.⁵ The DNA assembly bears a covalently tethered [Ru(bpy′)(dppz)(phen)]²⁺ (dppz = dipyridophenazine) and the 5′-GCGC-3′ protein-binding sequence at a distance of 14 base pairs away from the intercalation site of the ruthenium complex. In characterizing the spectrum of transient intermediates, the analogous assembly with non-covalently bound [Ru(phen)₂(dppz)]²⁺ was also employed. A 5′-GG-3′ sequence, the preferred site for oxidative damage,¹⁴ is not provided in this assembly. Instead, guanine residues flank an abasic site analogue within the protein-binding domain, 5′-

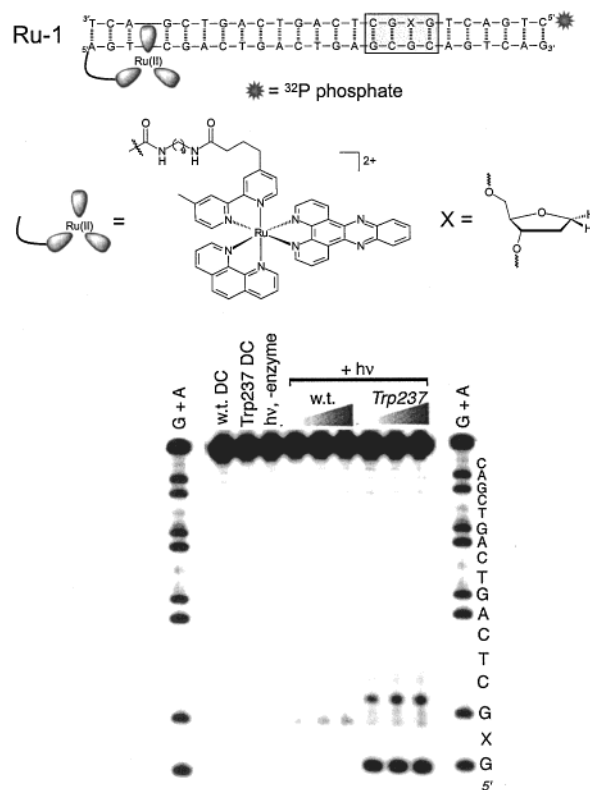


Figure 2. Photooxidative damage as a function of $M\cdot HhaI$ concentration and mutation. The 5′-³²P-end-labeled unmethylated DNA of duplex **Ru-1** as visualized by phosphorimaging following irradiation, piperidine digestion, and 20% denaturing polyacrylamide gel electrophoresis is shown. Irradiations were performed for 10 min at 436 nm using a 1000 W Hg/Xe lamp with monochromator at 25 °C. Reactions were carried out in the presence of either wild-type *M·HhaI* (lanes 5–7) or Q237W (lanes 8–10). Maxam–Gilbert G+A sequencing lanes are as noted. All reactions were 167 nM in **Ru-1** (based on duplex) in a total volume of 12 μ L. Enzyme concentrations were varied from 200 to 800 nM as denoted by the progressively thickened wedge above appropriate lanes. DNA–protein binding conditions were as described.¹⁵ All samples contained 25 mM NH₄OAc (pH 9.0), 1 mM KP_i (pH 7.4), 5 mM NaCl, 50 μ M EDTA, 5% glycerol, 200 nM SAH, and a 40-fold molar excess (in base pairs) of poly dA-poly dT. Dark control reactions (DC) contained 800 nM enzyme and 2 μ M [Ru(NH₃)₆]³⁺ but were not irradiated. Light control (*hv*, -enzyme) reactions consist of **Ru-1** subjected to irradiation conditions in the absence of protein.

GXGC-3′ (on the labeled strand); the insertion of the side chain of residue 237 is expected at this abasic site X upon protein binding.²⁴

Measurements of Oxidative Damage and of the Formation of Transient Intermediates. Figure 2 displays the gel electrophoretic results to characterize oxidative damage in assembly **Ru-1** as a function of protein binding and Figure 3 shows transient absorption results for **1**. As evident in Figure 2, no oxidative damage is apparent in the absence of protein. In the presence of wild-type *HhaI* methylase, a small extent of damage is found at the guanine 3′ to the abasic site, X. With bound Q237W mutant, however, extensive damage is evident 5′ to X, now the Trp insertion site. In our earlier studies with *HhaI* in rhodium-tethered assemblies, although oxidative damage was primarily observed at the 5′-GG-3′ doublets, some damage was observed also at the 5′-G to Trp insertion in the presence of mutant but not wild-type enzyme.¹⁵ We considered that this 5′-G reactivity may result from enhanced oxidation because of

(24) O’Gara, M.; Horton, J. R.; Roberts, R. J.; Xheng, X. *Nature Struct. Biol.* **1998**, *5*, 872.

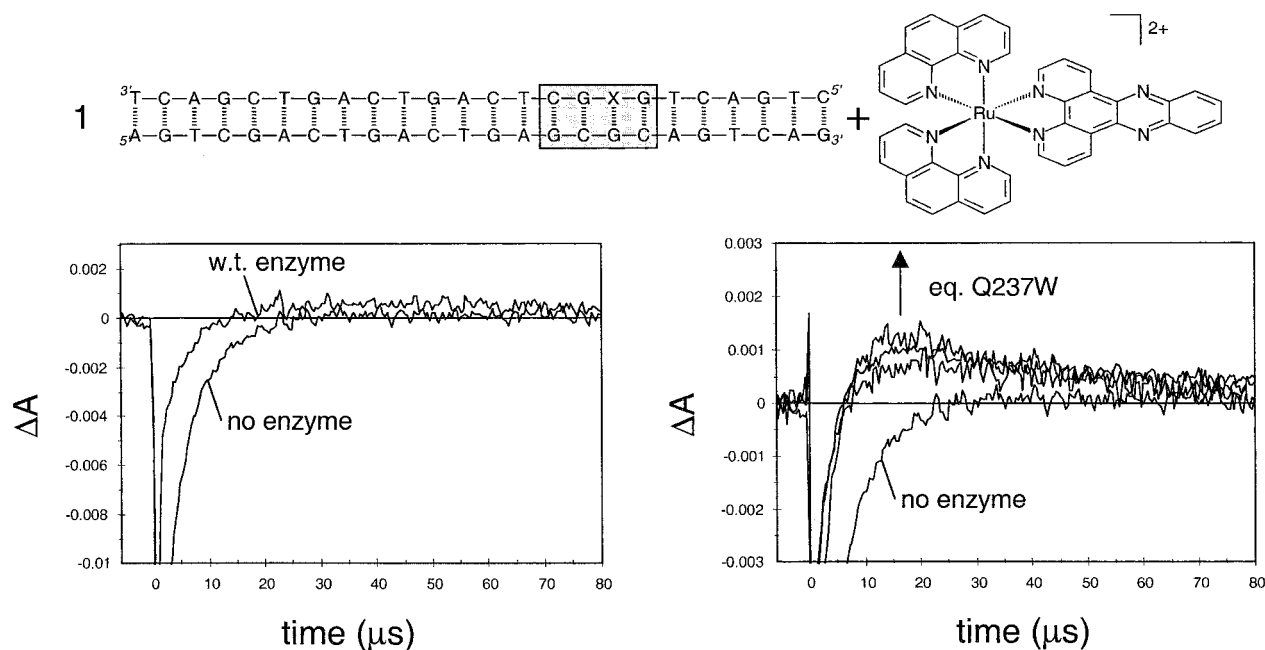


Figure 3. Transient absorption at 510 nm with formation of the transient intermediate with bound *M·HhaI* Q237W mutant but not wild-type enzyme. Samples contained oligonucleotide **1**, in the presence (15 μM) and absence of wild-type *M·HhaI* on the left and in the presence (3, 6, 12 μM) and absence of *M·HhaI* Q237W mutant on the right. Samples also contained $[\text{Ru}(\text{phen})_2(\text{dppz})]\text{Cl}_2$ (30 μM), **1** (30 μM), and $[\text{Ru}(\text{NH}_3)_6]\text{Cl}_3$ (3 mM) in 5 mM KP_i, pH = 9.0, $\lambda_{\text{exc}} = 480$ nm.

stabilization of the resultant guanine radical through stacking of the indole side chain to its 3'-side in a manner resembling stabilization of the 5'-G radical in guanine doublets by its 3'-G.¹⁴ The photochemical yield of this guanine damage is comparable to that found in ruthenated DNA assemblies containing 5'-GG-3' doublets ($\Phi = 10^{-3}$).¹⁸ Effective trapping of this guanine radical is not evident with wild-type enzyme, which lacks the Trp side chain, although the small extent of damage at the 3'-G suggests some radical formation at this 3'-G defect site.

To explore the formation of these proposed radical intermediates directly, transient absorption and emission spectroscopies were employed. On the basis of estimates of oxidation potentials, one might expect the formation of tryptophan as well as guanine radicals.²⁵ We examined first flash-quench reactions of duplex **1** with $[\text{Ru}(\text{phen})_2(\text{dppz})]^{2+}$ in the presence of *M·HhaI* Q237W (Figure 3). Excitation of $[\text{Ru}(\text{phen})_2(\text{dppz})]^{2+}$ bound to **1** by nanosecond laser pulses leads to an emission decay which can be fitted biexponentially.²⁶ This excited state is quenched efficiently by $[\text{Ru}(\text{NH}_3)_6]^{3+}$, with 90% quenching observed in the absence of protein and 85% in the presence of 0.5 equiv of protein (relative to **1**). In addition, *M·HhaI* Q237W does not quench the excited state of $[\text{Ru}(\text{phen})_2(\text{dppz})]^{2+}$, indicating the absence of direct electron transfer from the protein to $^*\text{Ru}(\text{II})$. We then assayed these assemblies by transient absorption spectroscopy at 510 nm, where a Trp radical is expected to show

Table 1. Experimental Details and Results of the Transient Absorption Experiments

DNA assembly	equiv ^a	rise (ΔA_{510})		decay (ΔA_{510})
		k_1 (s^{-1}) ^{b,c} (%)	k_2 (s^{-1}) ^b (%)	k (s^{-1}) ^d
1 ^e	0.1	5×10^6 (73)	3×10^5 (27)	2×10^4
1 ^e	0.2	5×10^6 (65)	3×10^5 (35)	2×10^4
1 ^e	0.4	6×10^6 (66)	3×10^5 (34)	1×10^4
1 ^e	0.5 ^f	10^6		
3 ^g	1.0	3×10^6		
Ru-5 ^h	1.0	5×10^6 (71)	3×10^5 (29)	1×10^4
Ru-4 ^h	1.0	5×10^6 (71)	2×10^5 (29)	1×10^4
Ru-1 ^h	1.0	5×10^6 (81)	2×10^5 (19)	1×10^4

^a Equivalents of *M·HhaI* Q237W relative to the amount of DNA.

^b Biexponential fitting of the signal. ^c These rates represent lower limits in the rise of the absorption signal, close to the instrument response for these experiments. Measurements at 440 nm on a faster time scale showed that the amount of Ru(II) increases within 100 ns, the excited-state lifetime, in the presence of *M·HhaI* Q237W; see ref 17 for details of the laser instrumentation. ^d Monoexponential fitting of the signal.

^e Samples contained 30 μM DNA, 30 μM $[\text{Ru}(\text{phen})_2(\text{dppz})]\text{Cl}_2$, 3 mM $[\text{Ru}(\text{NH}_3)_6]\text{Cl}_3$ in 5 mM KP_i, pH 9. ^f Equivalents of wild-type enzyme *M·HhaI*. ^g Samples contained 15 μM DNA, 15 μM $[\text{Ru}(\text{phen})_2(\text{dppz})]\text{Cl}_2$, 300 μM $[\text{Ru}(\text{NH}_3)_6]\text{Cl}_3$ in 5 mM KP_i, pH 9. ^h Samples contained 20 μM Ru-DNA, 3 mM $[\text{Ru}(\text{NH}_3)_6]\text{Cl}_3$ in 5 mM KP_i, pH 9.

maximum absorption.^{19,20,27} As evident in Figure 3, excitation of flash-quench samples containing DNA substrate **1**, $[\text{Ru}(\text{phen})_2(\text{dppz})]^{2+}$, and increasing concentrations of *M·HhaI* Q237W give rise to a transient absorbance formed within a few μs and decaying mostly within 100 μs (Table 1). Note that the transient rises first from a negative absorbance, reflecting the loss of Ru(III) as well as the gain of a new transient species. In the absence of *M·HhaI* Q237W, no transient species is detected, and this bleach recovery occurs with a rate of 10^4 s^{-1} . Interestingly, in the presence of wild-type *M·HhaI*, although no significant transient species is observed, the bleached signal recovers with a rate of 10^6 s^{-1} . Since these kinetics differ between mutant and wild-type enzymes, even though the quenching kinetics do not, this precludes back electron transfer from reduced quencher as being rate-limiting.

(25) The electrochemical potentials of guanosine ($E^{+/0} = 1.3$ V) and tryptophan ($E^{+/0} = 1.0$ V) were taken from Steenken, S.; Jovanovic, S. V. *J. Am. Chem. Soc.* **1997**, *119*, 617; Jovanovic, S. V.; Steenken, S.; Simic, M. G. *J. Phys. Chem.* **1991**, *95*, 684; see also Hush, N. S.; Cheung, A. S. *Chem. Phys. Lett.* **1975**, *34*, 11. The electrochemical potential of the Ru intercalator is $E^{3+/2+} = 1.6$ V; see Murphy, C. J.; Arkin, M. R.; Ghatlia, N. D.; Bossmann, S. H.; Turro, N. J.; Barton, J. K.; *Proc. Natl. Acad. Sci. U.S.A.* **1994**, *91*, 5315.

(26) Olson, E. J. C.; Hu, D.; Hormann, A.; Jonkman, A. M.; Arkin, M. R.; Stemp, E. D. A.; Barton, J. K.; Barbara, P. F. *J. Am. Chem. Soc.* **1997**, *119*, 11458.

(27) $\epsilon = 2.3 \times 10^3$ $\text{M}^{-1} \text{cm}^{-1}$ at 510 nm for the tryptophan radical according to Prütz, W. A.; Land, E. J. *Int. J. Radiat. Biol.* **1979**, *36*, 513. We assume a similar value for the DNA-bound radical.

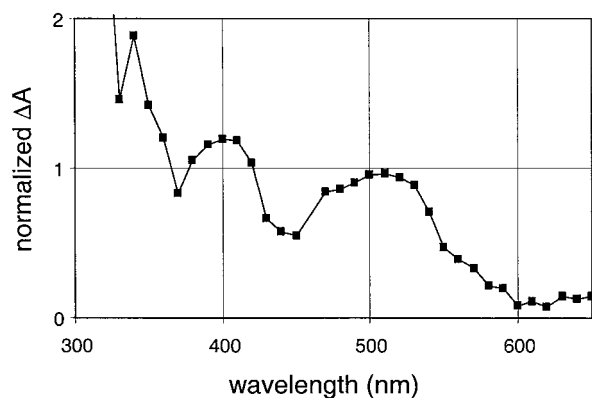


Figure 4. Transient absorption spectrum of the radical generated in flash-quench experiments using *M·HhaI* Q237W bound to DNA oligomers. The long-lived positive portion ($t > \tau^*(\text{Ru})$) of individual signals were fit to the monoexponential function $A(t) = C + A(t=0) \exp(-t/\tau)$, and $A(t=0)$ is shown plotted as a function of wavelength. The samples contained $[\text{Ru}(\text{phen})_2(\text{dppz})]\text{Cl}_2$ ($30 \mu\text{M}$), **1** ($30 \mu\text{M}$), *M·HhaI* Q237W ($15 \mu\text{M}$), and $[\text{Ru}(\text{NH}_3)_6]\text{Cl}_3$ (3 mM) in 5 mM KPi, pH = 9.0, $\lambda_{\text{exc}} = 470 \text{ nm}$.

To characterize more fully the intermediate formed in the presence of *M·HhaI* Q237W, the full absorbance difference spectrum was obtained (Figure 4). The spectrum has the same qualitative shape as that of the guanine radical in double-stranded DNA, with broad maxima at ~ 390 and $\sim 510 \text{ nm}$. However, for the neutral guanine radical, the 390 nm peak is about twice the height of the 510 nm peak,¹⁷ whereas these peaks are of similar height in Figure 4. We have obtained spectra of tryptophan radicals in flash-quench experiments using Lys-Trp-Lys previously, and while the spectrum of the Trp radical shows a broad maximum centered at 510 nm , it lacks a strong absorption at 390 nm .²⁰ Thus, the spectrum of the enzyme-dependent intermediate contains features both of the guanine radical (peaks at 390 and 510 nm) and of the Trp radical (peak at 510 nm). Given the spectral overlap between these two radical species, two interpretations are possible. The spectrum can be described as arising from a mixture of both guanine and tryptophan radicals, or could simply reflect an altered guanine radical spectrum with a change in the $A(390)/A(510)$ ratio. Note that the yield of this transient is comparable to that seen upon binding Lys-Trp-Lys¹⁹ and, moreover, corresponds roughly to that of irreversible guanine damage.

Inosine Substitution Experiments. We next sought to identify which guanine radical in the DNA assembly was being detected spectroscopically. While the gel electrophoresis experiments indicated clearly that only the guanine 5' to the abasic site was irreversibly oxidized, one might consider, especially in the context of a guanine hopping model,^{7,11} that guanine radicals along the path to irreversible oxidation were being generated as well. We therefore prepared assemblies **Ru-2** and **Ru-3** in which either the guanine 3' or 5' to the Trp insertion site was replaced by inosine. The oxidation potential of inosine is somewhat higher than that of guanine, owing to the absence of the minor groove exocyclic amino group.²⁵ Figure 5 shows the gel electrophoresis results for duplexes with and without inosine substitutions in the protein binding site. Significant oxidative damage is evident only in assembly **Ru-2** containing the sequence 3'-CIXG-5'. With assembly **Ru-3**, containing 3'-CGXI-5', the pattern of damage resembles that seen with **Ru-1** and wild-type enzyme.

The transient absorption measurements (Figure 6) provide a consistent picture. The transient absorbance formed at 375 nm with duplex **3**, lacking the 5'-G, showed a significant decrease

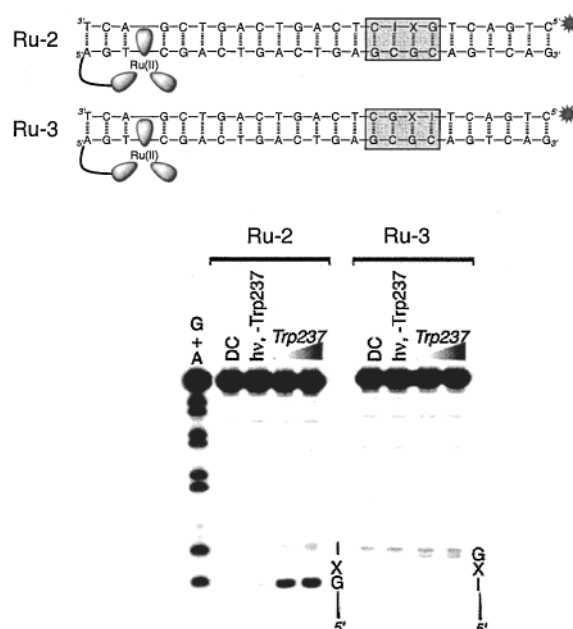


Figure 5. Denaturing polyacrylamide (20%) gel electrophoresis analysis of piperidine digests of duplexes **Ru-2** and **Ru-3** after flash-quench reactions in the presence of *M·HhaI* Q237W mutant. Duplexes used for each series of experiments are as noted above each series of lanes. Conditions and sample preparation are as given in Figure 2 and Experimental Section.

in intensity compared to that for 5'-GXGC-3'. In comparison, with duplexes **1** and **3** as substrates, the 510 nm signals differ less at early times and have the same height after $\sim 30 \mu\text{s}$. We attribute this equivalence at longer times to the presence of the tryptophan radical; the difference in absorption at earlier time may reflect the absorption by the 5'-G radical (for duplex **1**), which differs in its kinetics and also absorbs at 510 nm . These results then clearly support our assignment of the transient species formed for 5'-GXGC-3' sequences as stemming from a mixture of radicals, and furthermore identify the guanine radical being detected as that radical trapped 5' to the site of Trp insertion. Hence, while other guanine radicals may be generated transiently, they are short-lived.²⁸

Distance Dependence of Radical Formation. So as to examine the rate of formation of radical intermediates as a function of distance from the site of hole injection, the site of ruthenium intercalation, we prepared also DNA substrates **Ru-4** and **Ru-5** (Figure 7). All three DNA substrates **Ru-1**, **Ru-4**, and **Ru-5** contain a 5'-GCGC-3' sequence as the binding site for the protein with respect to the metalated strand. The complements contain the *M·HhaI* recognition sequence 3'-CGXG-5'. Distances of 24, 37, and 51 \AA are spanned from the sites of the intercalated metal complex to the G 5' to Trp insertion across the series **Ru-5**, **Ru-4**, and **Ru-1**, assuming 3.4 \AA stacking. As shown in Figure 7, gel electrophoretic analysis of damage showed that only a small variation in the yields of oxidative damage 5' to the inserted Trp is observed across this series of duplexes.²⁹ Similarly, as can be seen in Figure 8, flash-quench experiments revealed that the yield of the transient decreased somewhat with distance. Importantly, signals showed no significant variation in rate of formation of the transient.

(28) On this time scale, it is the neutral guanine radical that is detected. The guanine cation radical is shorter lived; possibly deprotonation (proton transfer to C) provides a basis for trapping. See S. Steenken *Free Rad. Res. Commun.* **1992**, *16*, 349 1992.

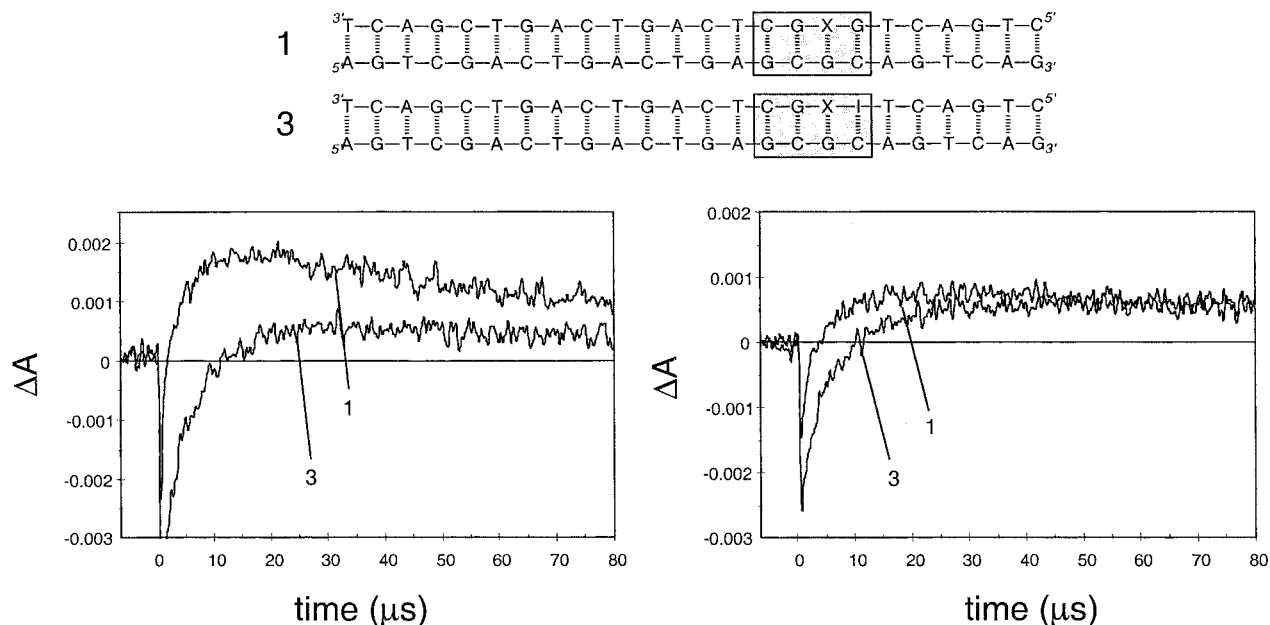


Figure 6. Transient absorption observed at 375 nm (left) and 510 nm (right), in the presence of *M·HhaI* Q237W mutant (20 μ M), using DNA duplex **1** or **3**. Samples contained DNA (15 μ M), $[\text{Ru}(\text{phen})_2(\text{dppz})]\text{Cl}_2$ (15 μ M), and $[\text{Ru}(\text{NH}_3)_6]\text{Cl}_3$ (0.3 mM) in 5 mM KP_i, pH = 9.0, $\lambda_{\text{exc}} = 470$ nm.

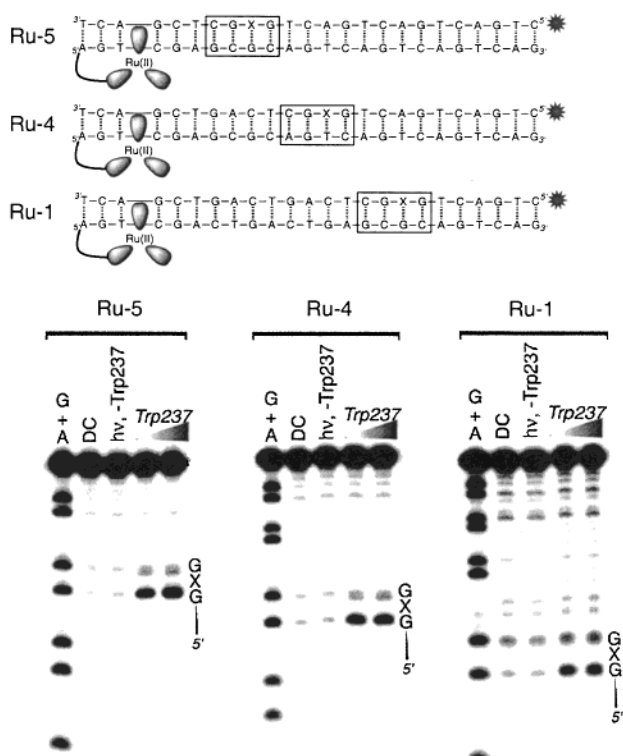


Figure 7. Denaturing polyacrylamide (20%) gel electrophoresis analysis of piperidine digests of duplexes **Ru-1**, **Ru-4**, and **Ru-5** after flash-quench reactions in the presence of *M·HhaI* Q237W mutant. Duplexes used for each series of experiments are as noted above each series of lanes. Maxam–Gilbert G+A sequencing lanes are as noted. Experimental details are as given in Figure 2. After flash-quench reaction in the presence of the Trp-containing mutant, significant oxidative damage is evident across the series **Ru-5**, **Ru-4**, and **Ru-1** at a distance of 24, 37, and 51 Å from the sites of metal to the G 5' to Trp insertion, assuming 3.4 Å stacking.

The formation of the transient clearly can occur no faster than the quenching process and, for the series, appears to be essentially synchronous with quenching in this time window.³⁰

Biexponential fitting of the rise of the intermediate yielded rate constants of $\sim 5 \times 10^6$ and $\sim 3 \times 10^5$ s⁻¹ for all three duplexes (Table 1). Hence, given the absence of a significant distance dependence in the rate of formation of transient species in the protein binding site, we conclude that hole transport through the DNA to the site of protein binding is not a rate-limiting process.

We assign the fast and slow components of the rate to injection of the electron hole into the DNA and the formation of radicals at the protein binding site, respectively. In duplexes **Ru-5**, **Ru-4**, and **Ru-1** with bound *M·HhaI* Q237W, the fast appearance of the positive 510 nm transient is synchronous with the ground-state recovery of the Ru(II) intercalator monitored at 440 nm, consistent with radicals being produced by a Ru(III) precursor. Moreover, duplex **3**, which lacks the 5'-G and significant guanine radical absorption, also exhibited this fast phase, but without a slower component. However, with either duplex **3**, lacking the G 5' to the Trp insertion site, or with wild-type enzyme, lacking an inserted Trp, the electron hole, once injected, is not trapped to yield a long-lived radical species; presumably back electron transfer or reduction of guanine radical by reduced quencher is rapid in these cases. We therefore assign this fast phase to hole injection. Stacking perturbations associated with the presence of a nonnative base, the indole side chain of the enzyme, into the DNA pocket, would make the trapping reaction of the radical within the protein binding site a slower process. We thus assign the slower component to formation of radicals at the protein binding site; the rate of hole transport across the 15–50 Å distance within the DNA duplex is then necessarily faster.

(29) Parallel analysis of DNA-protein binding by 10% native polyacrylamide gel electrophoresis revealed that Q237W bound with high efficiency ($\sim 70\%$ at $[\text{Q237W}] = 800$ nM) to duplexes **Ru-5**, **Ru-4**, and **Ru-1**.

(30) The value of the faster rate constant corresponds roughly to the instrumental response at the bandwidth used for this experiment. When measurements at 440 nm are carried out using a higher bandwidth and a shorter time window, it is evident that the amount of Ru(II) that recovers within 100 ns (the excited-state lifetime of the major emission component) increases in the presence of Q237W, consistent with the mutant enzyme facilitating fast injection of the electron hole into the DNA.

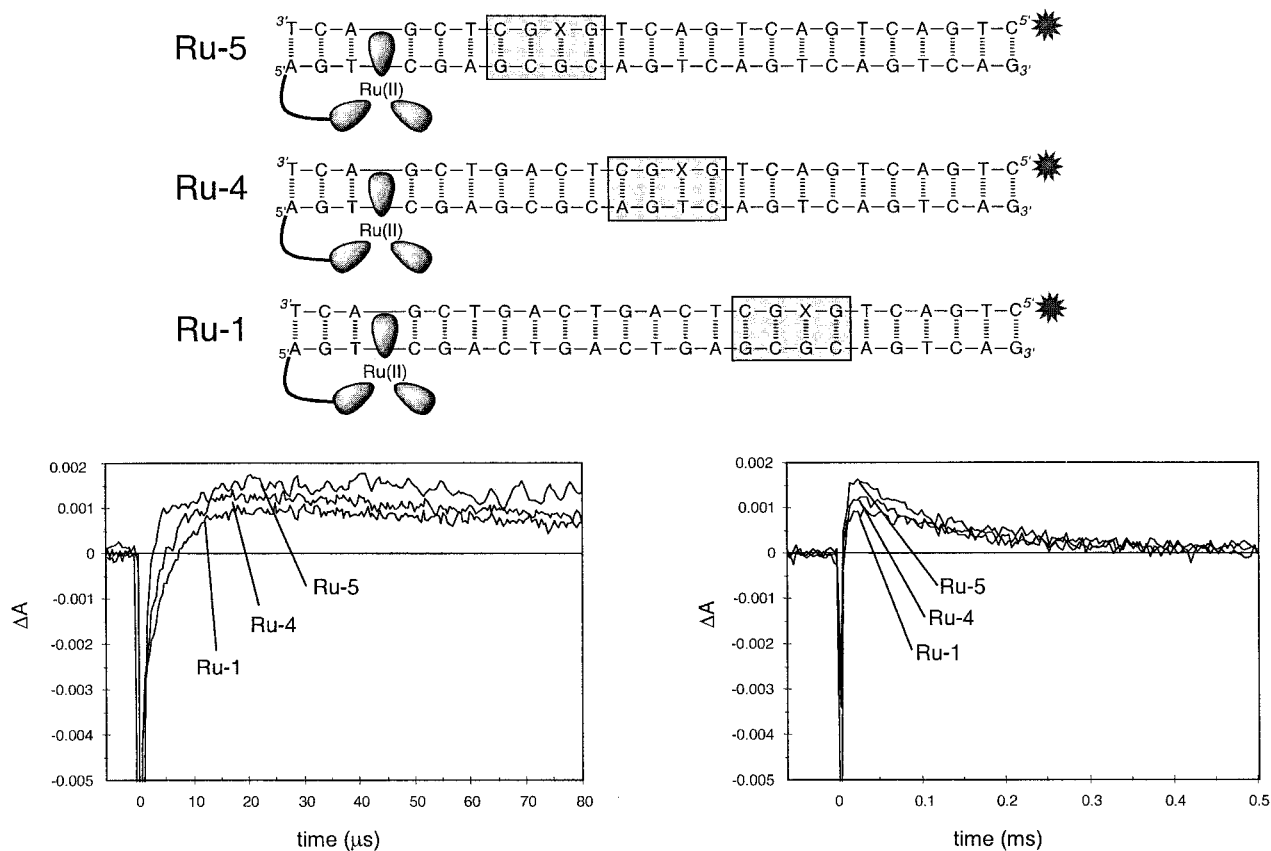


Figure 8. Transient absorption observed at 510 nm on two different time scales to show the rise (left) and decay (right) of the radical signals in the presence of *M·HhaI* Q237W mutant (20 μM) as a function of distance, using DNA duplexes **Ru-5**, **Ru-4**, or **Ru-1**. Samples contained Ru-DNA (15 μM), and $[\text{Ru}(\text{NH}_3)_6]\text{Cl}_3$ (0.3 mM) in 5 mM KPi , pH = 9.0, $\lambda_{\text{exc}} = 470$ nm.

Models for Charge Transport. On the basis of spectroscopic measurements, these experiments establish for the first time a lower limit on the rate of guanine radical formation within a DNA duplex as a result of DNA-mediated charge transport. These data furthermore establish directly the correlation between formation of the guanine radical and long-range oxidative damage, the former monitored spectroscopically and the latter monitored using gel electrophoresis. These data do not, however, provide information regarding the rate of a single hopping step nor the number of hopping steps required for transport across the 50 Å distance.

We can, however, view these data in the context of models proposed earlier. We first consider a guanine hopping model, involving hole transport among low-energy guanine sites.^{7,11} Inspection of the sequence for duplex **Ru-1** reveals the need, in the context of this model, for one intrastrand hopping step with two bases intervening between guanines, another with three bases intervening, and a third, with four high-energy bases intervening. A recent study by Lewis et al. indicated a rate of hole transport of $5 \times 10^7 \text{ s}^{-1}$ for intrastrand transport with only a single A intervening.¹⁰ If an exponential decrease in rate with an increase in the number of intervening higher-energy bases is as proposed by Lewis, we cannot reconcile our data with his value.³¹ Our study requires hole transport to be considerably faster.

Direct kinetic measurements have been carried out to determine rates of both intrastrand and interstrand charge transport using 2-aminopurine as the photoexcited electron acceptor with oxidation of either guanine or 7-deazaguanine.⁹ These low driving force reactions between modified bases do provide a consistent basis to understand the kinetics described here. Using these data, we expect the yield of coherent, single-

step transport over the 16 base pairs to be vanishingly small, owing to the dynamics of the intervening base stack. Hole transport, however, with three bases intervening, was observed in 200 ps; with four bases intervening, then, nanosecond rates might be expected. Alternatively, interstrand guanine hopping is possible, albeit with a penalty in rate of 10^3 as seen in comparing inter- and intrastrand rates. Four interstrand hopping steps with one base intervening as well as intrastrand hopping steps with a single A intervening would be required for our assembly; one might then estimate hops of 1–10 ns for each interstrand jump with a single base intervening. This estimate too would yield a rate for the overall transport process through the assembly that is faster and hence not competitive with rates of radical trapping. While these kinetic studies provide a plausible framework for viewing the data here, whether in fact hopping occurs among all the bases or among only guanine sites cannot be distinguished. Other models proposed for DNA-mediated charge transport, including polaron hopping⁶ or combinations in hopping and tunneling based upon thermal fluctuations in base pair stacking,⁵ necessitate rates which are fast compared to thermal relaxation in the DNA bridge. These models too would be satisfied by our experimental findings.

Implications. What the results described here clearly establish, thus far, therefore is a lower limit in rate of hole transport of $>10^6 \text{ s}^{-1}$ through 50 Å of the DNA base stack. Additional variations in sequence and length will be required to distinguish among models proposed. Moreover, these data, which combine

(31) For intrastrand transport between guanine sites, one expects the rate-determining step to be that between guanines with four intervening higher-energy bases. Extrapolating from Lewis' value of $5 \times 10^7 \text{ s}^{-1}$ for transport with one intervening A, and assuming on the basis of Lewis' data that $\beta = 0.7 \text{ \AA}^{-1}$,¹⁰ where according to Marcus theory,³² $k_1/k_2 = e^{-\beta(r_1-r_2)}$, one would predict that this single-step transport rate would be 10^4 s^{-1} .

and correlate biochemical studies of oxidative damage with spectroscopic measurements of the formation of transient intermediates, establish the validity of measurements of long-range oxidative DNA damage in reflecting guanine radical production and trapping. Moreover, we see that the decay of the neutral guanine radical, once trapped within the DNA duplex is slow, occurring on the 100 μ s time scale or slower. The molecular distances and time scales for long-range charge transport through DNA we have observed are therefore relevant to biological processes. Such long-range charge transport might conceivably play some role in the context of DNA repair processes and certainly requires consideration in evaluating patterns of oxidative damage to DNA in the genome.^{33,34}

(32) Marcus, R. A.; Sutin, N. *Biochim. Biophys. Acta* **1985**, *811*, 265.

(33) Rajsiki, S. R.; Jackson, B.; Barton, J. K. *Mutat. Res.* **2000** *447*, 49–72.

(34) Heller, A. *Faraday Discuss.* **2000**, *116*, 1–13.

Coupled with the demonstration that such transport can be modulated both negatively and positively by DNA-binding proteins, these observations therefore suggest the intriguing possibility that DNA-mediated charge transport chemistry may play a role in cellular processes.

Acknowledgment. We are grateful to the NIH (GM49216 to J.K.B.) for financial support. We also thank the Deutsche Forschungsgemeinschaft (H.A.W.) the Deutscher Akademischer Austauschdienst (M.P.), and the American Cancer Society (S.R.R.) for postdoctoral fellowships and Mount St. Mary's College Professional Development Fund and NSF (MCB981-7338) for funding of E.D.A.S. We are also very grateful to Drs. S. Kumar and R. J. Roberts of New England Biolabs for wild-type and Q237W mutant M•HhaI.

JA003986L